


# Grain-scale pressure variations and chemical equilibrium in high-grade metamorphic rocks

**Journal Article****Author(s):**

Tajcmanova, L.; Podladchikov, Y.; Powell, R.; Moulas, E.; Vrijmoed, J. C.; [Connolly, James](#) 

**Publication date:**

2014

**Permanent link:**

<https://doi.org/10.3929/ethz-a-010736091>

**Rights / license:**

[In Copyright - Non-Commercial Use Permitted](#)

**Originally published in:**

Journal of Metamorphic Geology 32(2), <https://doi.org/10.1111/jmg.12066>

**Funding acknowledgement:**

335577 - Interplay between metamorphism and deformation in the Earth's lithosphere (EC)

# Grain scale pressure variations and chemical equilibrium in high-grade metamorphic rocks

TAJČMANOVÁ L.<sup>1</sup>, PODLADCHIKOV Y.<sup>2</sup>, POWELL R.<sup>3</sup>, MOULAS E.<sup>1</sup>, VRIJMOED J.C.<sup>2</sup> AND CONNOLLY J.A.D.<sup>1</sup>

<sup>1</sup> *Department of Earth Sciences, ETH Zurich, Switzerland*

<sup>2</sup> *Department of Earth Sciences, University of Lausanne, Switzerland*

<sup>3</sup> *School of Earth Sciences, University of Melbourne, Vic. 3010, Australia*

Short title: Grain-scale pressure variation

## ABSTRACT

In the classical view of metamorphic microstructures, fast viscous relaxation (and so constant pressure) is assumed, with diffusion being the limiting factor in equilibration. This contribution is focused on the only other possible scenario—fast diffusion and slow viscous relaxation—and brings an alternative interpretation of microstructures typical of high grade metamorphic rocks. In contrast to the pressure vessel mechanical model applied to pressure variation associated with coesite inclusions in various host minerals, a multi-anvil mechanical model is proposed in which strong single crystals and weak grain boundaries can maintain pressure variation at geological timescales in a polycrystalline material. In such a mechanical context, exsolution lamellae in feldspars are used to show that feldspar can sustain large differential stresses (>10 kbar) at geological timescales. Furthermore, it is argued that the existence of grain-scale pressure gradients combined with diffusional equilibrium may explain chemical zoning preserved in reaction rims. Assuming zero net flux across the microstructure, an equilibrium thermodynamic method is introduced for inferring pressure variation corresponding to the chemical zoning. This new barometric method is applied to plagioclase rims around kyanite in felsic granulite (Bohemian Massif, Czech Republic), yielding a grain-scale pressure variation of 8 kbar. In this approach kinetic factors are not invoked to account for mineral composition zoning preserved in rocks metamorphosed at high grade.

**Keywords:** Diffusion, chemical zoning, equilibrium thermodynamics, mechanical equilibrium, pressure variation.

## INTRODUCTION

Mineral reactions are accompanied by volume and/or shape changes as well as changes in the chemical composition. In previous studies, emphasis has been placed on the separate roles of diffusion (e.g. Fisher, 1973; Joesten, 1977; Brady, 1983; Carlson & Johnson, 1991; Markl *et al.*, 1998; Milke & Heinrich, 2002; Keller *et al.*, 2008; Caddick *et al.*, 2010) or mechanics (Lee *et al.*, 1980; Morris, 1992, 2002; Fischer *et al.*, 1994; Liu *et al.*, 1998; Zhang, 1998; Mosenfelder *et al.*, 2000; Barron, 2003). However, stress and diffusion in solid phases are coupled (e.g. Stephansson, 1974; Fletcher, 1982; Wheeler, 1987; Schmid *et al.*, 2009) and, therefore, both the mechanical and the chemical response of a system should be considered together. Only limited information exists on the interplay between mineral reactions, chemical transport and pressure variations (Rutter,

1976; Ferguson & Harvey, 1980; Fletcher, 1982; Wheeler, 1987; Fletcher & Merino, 2001; Milke *et al.*, 2009; Schmid *et al.*, 2009). To address this shortcoming, the geological applicability of mechanical closure to account for petrographic observations of chemical zonation in high grade metamorphic rocks is investigated, in the case of zonation which cannot be explained fully by conventional, diffusion-based approaches (i.e. by sluggish kinetics).

During the pressure–temperature ( $P$ – $T$ ) evolution of a rock, mineral assemblages and compositions evolve until the process of equilibration becomes closed. There are two common mechanisms of reaction closure, thermal closure (Dodson, 1973) and mechanical closure (e.g. Chopin, 1984). As mentioned above, the role of mechanical closure in the interpretation of petrographic observations has only recently been recognised as being important (e.g. Schmid *et al.*, 2009). The classical thermal closure mechanism assumes that differences in chemical potentials are responsible for mass transport via diffusion, with diffusivities for each component generally being different. Diffusion rates then increase with temperature and even if equilibration volumes vary between different elements, mineral assemblages should be relatively well equilibrated on at least a millimeter scale at high temperature (say, above 750°C) at common geological timescales (Ma). Chemical equilibrium is realized when chemical potentials are equalized and diffusion stops. Thermal conduction and viscous stress relaxation are analogous to diffusion. At temperatures above 750°C, systems reach thermal equilibrium within seconds on a grain scale, thus rapid thermal relaxation is generally assumed in petrologic analysis (Fig. 1). Components like H<sub>2</sub>O, and Na<sub>2</sub>O, K<sub>2</sub>O and BaO have relatively high diffusivities, whereas the main constituents of most rock-forming minerals FeO, MgO, MnO, CaO and particularly SiO<sub>2</sub> and Al<sub>2</sub>O<sub>3</sub> have relatively slow diffusivities (Fig. 1). Given the small grain size of metamorphic matrix minerals the question arises as to why the chemical zonation in minerals at temperatures >750°C can be preserved in exhumed rocks.

Recent cooling or exhumation rate estimation based on diffusion modelling of chemical profiles have implied that these processes occur in bursts that are so short that they cannot even be resolved by traditional geochronological methods (Camacho *et al.*, 2005; Ague & Baxter, 2007), even if these rates appear to be geodynamically unrealistic, i.e. inconsistent with the regional geological context. Was the metamorphic process really so rapid with respect to diffusion that chemical equilibrium could not occur (the sluggish kinetics explanation)? Is it appropriate to use constant–pressure diffusion modelling for high–grade rocks with preserved chemical heterogeneities on a grain scale? Or is there another mechanism or controlling factor relating to the preservation of chemical zonation?

In classical diffusion modeling, which involves only chemical equilibration, the system is assumed to behave isobarically, i.e., that mechanical relaxation is infinitely fast. This assumption cannot be strictly valid in rocks with finite strength and viscosity. The behavior of a system can approach the isochoric or isobaric limit, depending on whether strength and viscosity are high or low respectively (Connolly, 1990; 2009). This might allow an explanation for the preservation of zonation at high temperature where diffusion

is fast; under such conditions the system is controlled mechanically. Considering this, stress relaxation, which is dependent on the viscosity of the rock, could potentially be calculated, but given how little is known about effective viscosities (Karato, 2003), the time for stress relaxation is indeterminate (Fig. 1a).

The present study addresses the effect of pressure variation in high-grade metamorphism. The focus is on accounting for the preservation of chemical zoning in crustal minerals at high temperature conditions (>750°C) where diffusional equilibration is expected to be rapid. An alternative model is built which is complementary to the idea of classical thermal closure. The only other possible scenario for reaction control is followed, as already suggested by Schmid *et al.* (2009), in which chemical diffusion is fast compared to viscous relaxation, with the strength of the minerals mechanically controlling maintenance of pressure variations. Then it is shown that grain-scale pressure variations can develop and that these pressure variations allow compositional zoning in minerals to be preserved at geological time scales. The results yield new insight concerning the preservation of mineral assemblages, mineral compositions and microstructures during high temperature metamorphism.

## **PRESSURE VARIATIONS AND MECHANICAL EQUILIBRIUM**

### **Pressure variation in metamorphic rocks—a classical pressure vessel example**

The preservation of coesite and diamond in a host mineral like garnet (Chopin, 1984), clinopyroxene (Smith, 1984) or zircon (Carswell, *et al.*, 2003) are well known examples where a high pressure inclusion is preserved during decompression (Rosenfeld, 1969; Zhang, 1998). The difference in pressure between the inclusion and the environment outside of the host has been shown by Parkinson & Katayama (1999) to be 20 kbar for coesite inclusions in garnet. The preservation of such a high-pressure phase as an inclusion is controlled by the strength of the host mineral (the pressure vessel model) which prevents the inclusion from transforming into the higher-volume lower-pressure polymorph (Gillet, *et al.*, 1984; van der Molen & van Roermund, 1986; Morris, 1992; Liu *et al.*, 1998; Zhang, 1998; Mosenfelder *et al.*, 2000; Ye, *et al.*, 2001; Barron, 2003; Chopin, 2003; Guiraud & Powell, 2006; O'Brien & Ziemann, 2008). However, the pressure vessel model is inappropriate for a polycrystalline rock involving weak grain boundaries and relatively strong single crystals. For these cases, a different mechanical representation of the system is needed.

### **Pressure variation in polycrystalline material—a multi-anvil model**

Forces acting upon objects in mechanical equilibrium are balanced. By definition, stress ( $\sigma$ ) is equal to force ( $F$ ) per unit area ( $A$ )

$$\sigma = \frac{F}{A} \quad (\text{Eq. 1})$$

Therefore, the force balance does not require a balance of stresses due to area variations. For example in a piston cylinder apparatus, stress in the thinner part of the pillar (smaller area) is significantly amplified while maintaining force balance (Fig. 2a). Similarly, in an effectively spherical multi-anvil apparatus (Fig. 2b), the inner stress is amplified proportionally to the radius squared while maintaining radial force balance. At every

point in solids, the value of the normal stress depends on its orientation and ranges between maximum and minimum stresses,  $\sigma_{max}$  and  $\sigma_{min}$  respectively. For example in a piston cylinder apparatus, the vertical stress is different from the horizontal stress at every point of the system. In general, the difference between  $\sigma_{max}$  and  $\sigma_{min}$  controls deformation (change of shape), whereas mean stress is associated with volume change of the solids. Thermodynamic (metamorphic) pressure must lie between  $\sigma_{max}$  and  $\sigma_{min}$  (i.e.  $\sigma_{min} < P < \sigma_{max}$ ). The difference between  $\sigma_{max}$  and  $\sigma_{min}$  is commonly assumed to be negligible (Fig. 3a).

Considering the spherical inclusion–host environment, in radial coordinates,  $\sigma_{max}$  corresponds to the radial stress and  $\sigma_{min}$  to the circumferential stress (Fig. 3). In such a case, force balance is satisfied if

$$\frac{d}{dr} \sigma_{max}(r) + \frac{2(\sigma_{max}(r) - \sigma_{min}(r))}{r} = 0 \quad (\text{Eq. 2})$$

where  $r$  is the radial coordinate. Because Eq. 2 relates two unknown components of the stress, a rheological constitutive assumption is needed to define the stress profile in the host.

Different stress and pressure profiles arise for two possible end–member rheologies, namely pre–failure linear elastic or linear viscous rheology (the pressure vessel model) and a post–failure rheology with weak radial grain boundaries (the multi–anvil model). These end–members are illustrated for a spherical inclusion–host system with radial coordinate  $r$  in Fig. 3b–d. For the elastic or viscous rheology, the differential stress in the host ( $\sigma_{max} - \sigma_{min}$ ) can be large, but, interestingly, the mean stress ( $\bar{\sigma}$ ) distribution is constant across the host (Fig. 3b). The stress difference,  $\sigma_{max} - \sigma_{min}$ , in the host decreases with distance towards the matrix as  $1/r^3$  (Fig. 3b). The maximum value of the differential stress in the host next to the inclusion is 1.5 times higher than the pressure difference between the inner and outer part. If the pressure difference is high (>10kbar), the maximum differential stress would be 1.5 times higher leading to a failure, i.e. the development of radial cracks. The fully disintegrated end–member assumes complete failure of the grains adjacent to the inclusion along radial grain boundaries while the radial stress gradients inside the grains are still maintained. This configuration of strong crystals with weak grain boundaries is referred to as the multi–anvil model (Fig. 3c, d). In this case, circumferential force balance requires  $\sigma_{min} = P_{\infty} = \text{const.}$  (see Fig. 3c) and radial force balance satisfies

$$\frac{d}{dr} \sigma_{max}(r) + \frac{2(\sigma_{max}(r) - P_{\infty})}{r} = 0 \quad (\text{Eq. 3})$$

Solving (3) for  $\sigma_{max}(r)$  with boundary condition  $\sigma_{max}(r_{inc}) = P_{inc}$  (Fig. 3c) results in

$$\sigma_{\max}(r) - P_{\infty} = (P_{inc} - P_{\infty}) \frac{r_{inc}^3}{r^2} \quad (\text{Eq. 4})$$

where  $r_{inc}$  and  $P_{inc}$  are the radius and pressure of the inclusion, respectively. In contrast to the elastic case, the stress difference  $\sigma_{\max} - \sigma_{\min}$  and mean stress ( $\bar{\sigma}$ ) decreases from the inclusion towards the matrix as  $1/r^2$  (Fig. 3d). The stress dependence on the radius can be rearranged to a more intuitive expression of force balance:

$$F(r) = P_{op}(r)A(r) = P_{op}(r_{inc})A(r_{inc}) = F(r_{inc}) \quad (\text{Eq. 5})$$

where  $A$  is the area of sphere,  $P_{op}$  is the overpressure over the matrix pressure from Eq. 4 ( $\sigma_{\max}(r) - P_{\infty}$ ). Equation 5 shows that force balance (i.e. mechanical equilibrium) does not require zero stress gradients. This phenomenon is exploited, for instance, in the multi-anvil apparatus to amplify and maintain the externally applied pressure. Thermodynamic pressure is thought to be equal to either the radial stress (Kamb, 1961; Paterson, 1973; Wheeler, 1987) or the mean stress (Dahlen, 1992). In either case, the thermodynamic pressure is not constant radially (compare Fig. 3a and 3d), even within a weak polycrystalline rim encircling a high pressure inclusion. This multi-anvil representation corresponds better to natural observations of polycrystalline microstructures than the purely elastic pressure vessel model. However, the most important observation is that in both model end-members—strong (pressure vessel) and weakened due to grain boundaries (multi-anvil)—pressure variations can be sustained. Therefore, even if in reality natural samples correspond to a rheology lying between the two end-members, the possibility that pressure variation can be maintained at geological timescales cannot be ruled out if the viscous relaxation within the strong grain is slow compared to its homogenization by diffusion. Observations of such a pressure variation in natural samples have become more common recently (e.g. Zhang & Liou, 1997; Endo *et al.*, 2012; Moulas *et al.*, 2013) and, as a result, the necessity for an explanation for this phenomenon has arisen. More complex mechanical models, for example, for spherical cavity expansion in rock masses, are also available and their applicability has already been described in detail by, for example, Yu & Houlsby (1991), Yu (2000) and Yarushina & Podladchikov (2010). However, these models are beyond the scope of this study due to their complexity and the number of necessary constitutive parameters.

Materials can be strong or weak depending on composition and fluid/melt presence (Robertson, 1955; Brace, 1970; Ji *et al.*, 2000; Rybacki & Dresen, 2000; 2004; Mancktelow, 2008; Moghadam *et al.*, 2010). Resistance of a rock to deformation is also dependent on the geometric configuration of a system. In the multi-anvil model, maintaining pressure variation is mechanically feasible for any rheology of the grain boundary (e.g. reaction rims). Furthermore, if the anvils are solid solutions, then the mechanically-maintained variation in thermodynamic pressure (bounded by  $\bar{\sigma} < P < \sigma_{\max}$ ; Fig. 3d) results in radial chemical zoning. In this model, the radial quasi steady-state pressure variation is likely to cause a redistribution of components, with higher density end members diffusing towards the high pressure (inner) side of the anvil.

At chemical equilibrium, a chemical zonation is present as long as the pressure gradient is maintained.

### **AN ALTERNATIVE APPROACH—UNCONVENTIONAL BAROMETRY**

The preservation of composition and pressure variations is a consequence of how both the diffusional and the mechanical closure is attained. The quantification of a pressure profile from the foregoing mechanical model is impractical given the uncertainties related to strength constraints mentioned above. Therefore, an alternative approach to the prediction of pressure profiles in single grains that is independent of the rheology parameters is required. Here such an approach is developed, based on equilibrium thermodynamics, that accounts for chemical heterogeneities in solid solutions mutually connected with high–pressure minerals observed in thin section such as coesite or kyanite.

Under general conditions, including the presence of pressure gradients, chemical equilibrium within a phase is represented by the assumption of zero net flux across the microstructure. Considering a binary system involving two components, A and B, i.e. with only one independent component, the difference between the chemical potentials of the two components is constant in space (Loomis, 1978)

$$\Delta\mu = \mu_A - \mu_B = \text{const.} \quad [\text{Eq. 6}]$$

Under such conditions, the commonly–observed chemical zonation in high–grade phases should be removed. Therefore it is assumed that chemical variations in grains which are attached to a high–pressure phase and associated with decompression from high pressure at higher temperature can be preserved only by reflecting pressure variations on that scale, as a consequence of attaining mechanical equilibrium (Fig. 4a). In fact, such an equilibrium in a pressure gradient can be used as an unconventional barometer. The following derivation is for a binary system with components A and B. In this approach, temperature is assumed to be constant across a given microstructure as thermal equilibration is the fastest process involved (Fig. 1).

The approximate equilibrium relation (6) is converted from molar to the exact mass form to satisfy the mass conservation, involving the  $\Delta\mu$  written in terms of chemical potentials normalised to molar mass,  $M_i$ , following, for example, Gibbs (1906), Truesdell (1962), Landau & Lifshitz, (1987), de Groot & Mazur (1962), Kuiken (1994) and Müller & Weiss (2012).

$$\Delta\mu = \frac{\mu_A}{M_A} - \frac{\mu_B}{M_B} = \text{const.} \quad [\text{Eq. 7}]$$

Expanding (7), at constant  $T$ , but allowing  $P$  to vary, gives

$$\frac{\mu_A}{M_A} - \frac{\mu_B}{M_B} = \left( \frac{PV}{M_A} + \frac{RT \ln a_A}{M_A} \right) - \left( \frac{PV}{M_B} + \frac{RT \ln a_B}{M_B} \right) \quad [\text{Eq. 8}]$$

where  $P$  is pressure,  $V$  is molar volume,  $R$  is gas constant,  $T$  is temperature,  $M$  is molar mass and  $a_A$  and  $a_B$  are activities of components A and B. In (8), the constant terms in the definition of the chemical potentials have cancelled.

If the chemical potential difference is constant across a zoned rim or porphyroblast (Fig. 4a), in the sense of Eq. 7, a pressure change imitating the compositional change across the grain is required to maintain the force balance (Fig. 4a). The assumption is that each compositional step in the zoned profile across the grain can be taken as a point on a parabola for which Gibbs free energy (chemical potential) is known at given pressure and temperature. Under pressure gradients at constant temperature, chemical potentials are changing and thus different points on a parabola will be stable at each pressure step following the compositional changes across the grain (Fig. 4b). Each step on the  $G$  surface involves the phase at  $P1$  being in equilibrium with its neighbor at  $P2$ , with zero flux

$$\left( \frac{\mu_A}{M_A} - \frac{\mu_B}{M_B} \right)_{P1} - \left( \frac{\mu_A}{M_A} - \frac{\mu_B}{M_B} \right)_{P2} = 0. \quad [\text{Eq. 9}]$$

This is represented by the dashed arrow (Fig. 4b).

The observed chemical profile can serve as a barometer (Fig. 4a) by setting

$\frac{\mu_A}{M_A} - \frac{\mu_B}{M_B}$  for one pressure, equal to  $\frac{\mu_A}{M_A} - \frac{\mu_B}{M_B}$  for another, the difference in pressure is

$$\Delta P = \frac{RT \left( \frac{\ln(a_A)_{P2} - \ln(a_A)_{P1}}{M_A} - \frac{\ln(a_B)_{P2} - \ln(a_B)_{P1}}{M_B} \right)}{\left( \frac{V_B}{M_B} - \frac{V_A}{M_A} \right)} \quad [\text{Eq. 10}]$$

where the activities of A and B are at  $P2$  and  $P1$  respectively. The result obtained then represents the dependence of pressure difference on the concentrations. Applying Eq. 10 to the measured concentration profiles in the minerals studied yields relative pressure differences. If the calculated pressure profile based on equilibrium thermodynamics is compared with the qualitative pressure profile in the mechanical model described above (Fig. 3d) and the denominator in Eq. 10 is expressed in terms of density  $\left( \frac{1}{\rho_B} - \frac{1}{\rho_A} \right)$ , the

prediction that the higher density end member occurs at the higher pressure (inner) side of the anvil is satisfied.

## EXAMPLES

Two examples of high-grade microstructures, which can be found within a single thin section, were chosen in order to discuss the evidence for preserved pressure variations on a grain-scale (Fig. 5). The first example of exsolution lamellae in alkali feldspar documents that feldspar can sustain stresses up to 20 kbar at geological timescales. The



second example of plagioclase rims on kyanite illustrates that pressure variation is a valid explanation for microstructures involving preserved composition zoning commonly ascribed to disequilibrium.

Figure 5 is a sketch based on the observations of microstructures in high-pressure felsic granulites from the Bohemian Massif (Variscan belt of Central Europe) described in detail by Štípská *et al.*, (2010), Franěk *et al.* (2011) and Tajčmanová *et al.* (2011). These rocks are mostly characterized by a Grt–Ky±Bt–Pl–Kfs–Qtz mineral assemblage corresponding to peak  $P$ – $T$  conditions of 16–18 kbar and 850–900°C followed by nearly isothermal decompression (Franěk *et al.* 2011; Tajčmanová *et al.*, 2011). The description of the compositions of the phases involved, and discussion of the details of the  $P$ – $T$  evolution is beyond the scope here. They can be found in the works referred to above.

### **Exsolution lamellae in alkali feldspars**

A simple example of pressure variation on a grain scale is provided by coherent exsolution lamellae. They are a typical microstructure in alkali feldspar that is generated by precipitation of a more albite-rich phase from alkali feldspar or ternary feldspar of an intermediate composition during cooling, producing at the same time a more orthoclase-rich host (Fig. 6). Already in the 1970s, transmission electron microscope observations documented coherent lamellae in alkali feldspars in which the lamellae maintain full continuity of their lattices across the lamellar interfaces (Brown & Willaime, 1974; Willaime & Gandais, 1972; Robin, 1974). In particular, Robin (1974) documented that coherency causes elastic strains in the individual lamellae affecting the lattice parameters. For a very small proportion of pure coherent albite lamellae within an orthoclase grain, the values for stress correspond to 6 kbar parallel to the  $b$ -axis and 23 kbar orthogonal to  $b$ -axis (Robin, 1974). Values, of 9 and 20 kbar, were obtained for a coherent albite precipitate in microcline (Pryer & Robin, 1996). Moreover, the coherency stresses in alkali feldspars may be even higher when updated elastic constants are used (Neusser *et al.*, 2012). These results are not surprising if the volume difference between the orthoclase-rich feldspar and albite-rich precipitate (up to 10 vol%) is taken into account. These nanometer-scale pressure variations due to the volumetric change at the precipitate–host interface are comparable to the case of coesite inclusions in garnet.

In slowly-cooled rocks, the exsolution lamellae are often incoherent, most likely a consequence of stress relaxation (the partial or complete release of the induced pressure variations) involving destruction of an original coherent perthitic microstructure. In Example 1 (Fig. 5, 6), where two generations of exsolution lamellae are present, the first generation of lamellae, corresponding to higher-temperature exsolution (800°C; Tajčmanová *et al.*, 2012), is already incoherent, but the lower temperature (680°C; Tajčmanová *et al.*, 2012) second generation is still coherent (Fig. 6). Given the elastic constants for alkali feldspars and the coordinate system used in Robin (1974), the stress was calculated for directions parallel (13–18 kbar) and orthogonal (6–8 kbar) to the  $b$  axis based on the chemical composition of the precipitate (Fig. 6). The fact that the perthitic microstructure is still preserved reflects the fact that even feldspar as a representative of an apparently weak material can sustain large stresses internally at geological timescales.

### **Plagioclase rims on kyanite**

The second example offers an alternative explanation of a reaction rim microstructure around a high-pressure phase which is a very common feature in high-grade kyanite-bearing rocks. Plagioclase rims around kyanite grains have a radial thickness from 50 up to 200  $\mu\text{m}$  depending on their microstructural position. They are present both in the polycrystalline matrix and in large perthite grains (Fig. 5; 7). The plagioclase rim may comprise either by a single grain or it can be polycrystalline with grains of different crystallographic orientation (Tajčmanová *et al.*, 2011). Regardless of this, the plagioclase rims show identical continuous outward decrease of the anorthite content ( $\text{Ca}/(\text{Ca}+\text{Na})$ ; mol%) from  $\text{An}_{35}$  at the contact with kyanite to  $\text{An}_{20}$  at the contact with the surrounding matrix. Such a zonation has been explained by sluggish kinetics involving the slow diffusion of Al (Tajčmanová *et al.*, 2007; Štípská *et al.*, 2010). Taking into account the high-grade  $P$ – $T$  conditions during which the plagioclase rim grows, about 800°C, and the scale on which the microstructure is preserved, all components should have been already equilibrated within a few hundred thousand years (see Discussion and Conclusions below). However, this interpretation conflicts with the duration of the decompression event estimated at around 10 Ma from geochronology (details in Franěk *et al.*, 2011).

The plagioclase rim can be described by the binary albite–anorthite chemical system. For such a system at constant temperature, zero fluxes can be calculated at given pressures using Eq. 10 with the feldspar activity model of Holland & Powell (2003), based on the compositional changes across the plagioclase rim (Fig. 9a). The result based on the direct data indicates that the overall equilibrium is satisfied only when pressure variations are considered. If the isobaric assumption is made, the  $\Delta\mu$  (Eq. 7, 8) is never constant (Fig. 8). Therefore, following the alternative explanation described above based on the assumption of overall chemical equilibrium and force balance, the preserved chemical zonation within the rim is inferred to be the result of pressure variation. Pressure changes progressively across the plagioclase rim from higher pressure in the kyanite to lower pressure in the matrix (Fig. 9a,c). This is also supported by the fact, that more anorthite-rich compositions at the kyanite interface have higher density (and thus indicate higher pressure) than the more albitic ones at the matrix interface (Fig. 9b). The surrounding matrix, being composed of quartz and K-feldspar, show little or no compositional zonation, and thus documenting of any pressure variation into the matrix is not possible. The compositional profile can be used as a barometer and the total pressure difference between both interfaces of the rim corresponds to around 8 kbar (Fig. 9c). This means that, after the decompression of the rock, say to 10 kbar, the pressure in the kyanite is still at 18 kbar, with pressure decrease across the plagioclase rim from 18 kbar to 10 kbar.

## **DISCUSSION AND CONCLUSIONS**

### **Microstructure diversity—the limits of the application of the present model**

An alternative explanation for chemical zoning in porphyroblasts and reaction rims preserved in high-grade rocks has been outlined. An alternative model is required because the classical approach based on thermal closure does not fully explain the petrographic observations described above. Furthermore, a model based on fast diffusion and slow viscous relaxation, which would be complementary to the classical view as suggested by Schmid *et al.* (2009), had not been applied to natural samples. The approach

used here avoids invoking the sluggish kinetics interpretation commonly used in accounting for preserved mineral zonation in high-grade rocks. Also, the approach accounts for local chemical heterogeneities which, based on regional geology data, are unlikely to be connected with very fast geological processes such as exhumation or local short thermal pulses that have been proposed to account for them (e.g. Camacho *et al.*, 2005; Ague & Baxter, 2007).

The alternative approach does not attempt to account for the mechanisms which are responsible for the growth of the precipitates in perthitic feldspar or the growth of the plagioclase rim. These require a consideration of the rheology of the developing microstructure and its surrounding with time, and are beyond the scope of this paper. Because the approach used here is an inverse model it only focusses on explaining why a microstructure or a compositional zonation is preserved at high temperature. Therefore, the thermodynamic approach is applicable to all petrographic observations where a high-pressure assemblage/phase is separated from a low pressure assemblage/phase by a zoned mineral, independent of any rheology parameters.

Two different microstructures were described in order to discuss pressure heterogeneity on the thin section scale. The exsolution lamellae from Example 1 vary from nanometer scale to a maximum of a few micrometers, thus the size of the confined space here is mostly on a lattice scale which is very stiff. The most evident are precipitates in feldspars from volcanic rocks that were cooled down very quickly allowing preservation of coherent lamellae (e.g. Robin, 1974). However, exsolution lamellae in feldspar also provide a very important documentation of pressure variation in regionally metamorphosed rocks at geological timescales. Considering the two generations of exsolution outlined above in slowly cooled samples, large stress variations in exsolution lamellae were obtained for the second coherent generation (Fig. 6), as similarly documented by Robin (1974). Assuming the  $\bar{\sigma} < P < \sigma_{\max}$ , the values of stresses in albitic precipitates (Fig. 6) would imply metamorphic pressure variations between 13 and 18 kbar. In contrast, pressure variations for the incoherent generation should have diminished, even though the shape of the first generation lamellae is still preserved. The elastic constants used for the calculation of induced stresses are for alkali feldspars. However, the first generation of precipitates was developed in the system involving CaO. Given that the content of anorthite component in the integrated composition of the feldspar is very low (5 mol% anorthite; Tajčmanová *et al.*, 2012), its effect on elastic properties and hence the resulting stress values is assumed to be negligible. The metamorphic pressure variation for the first generation of precipitates is estimated at around 10 kbar.

These results show that the induced pressure variations inside the large feldspar grains were enormous on the nano- to micrometer scale and were sustained over geological time scales. Furthermore, it is interpreted here that the reason why the spatially well-organized microstructure was not immediately fully transformed into a new coarse-grained phase with lower Gibbs energy is that it is mechanically maintained, preventing it from being completely recrystallized.

The plagioclase rims around kyanite grains were also developed at high temperature during decompression (800°C; Štípská *et al.*, 2010; Tajčmanová *et al.*, 2011). No matter which mechanism was responsible for their growth, the chemical zonation is still well preserved. There are two different thicknesses of the rims connected with different microstructural position in the same thin section, 50 and 150 µm, respectively, in the samples studied by Tajčmanová *et al.* (2011). Taking into account the coefficient for CaAl–NaSi interdiffusion in plagioclase for dry systems at 800°C ( $10^{-22}$  m<sup>2</sup>/s; Yund, 1986; Liu & Yund; 1992; Korolyuk & Lepezin, 2009; Cherniak, 2010), the removal of such zoning in plagioclase (in a layer with a thickness of 100 µm) should have been complete in  $\ll 0.5$  Ma. This duration is unlikely from a tectonic point of view for this region, so the survival of the zoning needs to be explained. Moreover, if classical diffusion theory was applied here (with no pressure variation), given different thicknesses of the rims and same compositional differences within one thin section, different durations of equilibration would be inferred.

The suggested incorporation of mechanical equilibrium provides a more elegant and physically defensible explanation than the speculative mechanism of sluggish kinetics. The plagioclase rim then reflects a steady state long duration process, based on the whole microstructure being in mechanical and chemical equilibrium. If there is a pressure gradient across the profile, the equilibrium conditions are reflected in a trend of isopleths with constant difference in chemical potentials (Fig. 8a). If an isopleth is followed, the way that pressure varies across the profile is given.

The multi-anvil model (strong single crystal and weak grain boundaries) leads to the preservation of the chemical zonation inside the single crystal as long as it survives against processes such as deformation, fluid infiltration or a sudden increase of temperature. Survival may be for a long time, e.g. millions of years, which would then be consistent with results from conventional geochronology for the region studied. The identical chemical zonation is not only for different thicknesses of the plagioclase rim but also for different crystallographic orientations in either the single crystal or the polycrystalline rim. This supports the multi-anvil mechanical concept allowing for maintaining pressure variations also in polycrystalline material and not only for homogeneous grains such as garnet (as for coesite inclusions).

As a comparison, pressure variation in coesite/garnet example can correspond to 20 kbar (e.g. Parkinson & Katayama, 1999; O'Brien & Ziemann, 2008). In the example of the plagioclase rims around kyanite, a smaller pressure variation (8kbar) is obtained. This pressure difference is significantly less than those retrieved from inclusion–host relationships in UHP rocks based on the classical pressure vessel model, but it is feasible regarding the rheology studies on stress relaxation and strength of feldspars (Rybacki & Dresen, 2000; 2004) and in polyphase rock aggregates (Ji *et al.*, 2000). Regardless of the rheology data, perthite with incoherent exsolution lamellae can be considered as a polycrystalline material (two different phases, dislocations). Then the preservation of a second generation of coherent exsolution lamellae in one feldspar grain already weakened by the first generation of incoherent exsolution lamellae documents directly a

minimum feldspar strength of 10 kbar at geological time scales and temperatures around 650–700°C .

### **Implications for estimation of $P$ – $T$ and rates of metamorphic processes**

There are several potentially important implications of the proposed mechanical point of view. Estimation of the rates of metamorphic processes via diffusion modeling without considering the consequences of a mechanical equilibrium is likely to be misleading, especially for high temperature rocks. Also the corollary, using microstructures to deduce diffusion coefficients when the thermal story is known, may seriously under-estimate coefficient values. As shown above, taking into account mechanical equilibration suggests that pressure variations correspond to chemical variations (Fig. 4). The rate controlling factor is always the slowest (Schmid *et al.*, 2009) and, at high temperatures, diffusion is fast. This new view regarding what is preserved in high-grade rocks is unlikely to mean that the evolution of the rock, such as burial or exhumation, must have been so fast that it did not have time to chemically equilibrate. However, below 650°C, at conditions typical for example for Barrovian metamorphism, the possibility that conventional rate estimates are valid cannot be excluded.

In phase equilibria calculations, the application of equilibrium thermodynamics requires a careful estimate of equilibration volume because of the apparent limited scale of equilibration especially at fluid-deficient conditions. Clearly the possibility of grain-scale pressure variations affects how rocks should be considered using a phase equilibria modeling approach. If pressure variations are present, they should preclude the use of  $P$ – $T$  diagrams calculated for a bulk rock composition where those variations are deduced to occur, unless the whole microstructure in which pressure variation is involved is excluded from the bulk composition. In many studies, small chemical and by interference possible pressure variations in the thin section are commonly neglected. However, the observation of such local chemical variations is very important for understanding all processes which took place in the sample and should not be ignored. For the phase relationships which involve large volumetric changes, the  $V$ – $T$  diagram at constant pressure can be informative in understanding the chemical equilibrium processes (e.g., Connolly, 1990, 2009; Powell *et al.*, 2005). Such diagrams are helpful in a qualitative way in studies of, for instance, melting processes, but they cannot portray the pressure variations transparently as the mechanical equilibrium is not included in the approach.

In thermobarometry, chemical zoning in minerals is generally believed to be inappropriate for use in determining  $P$ – $T$  estimates due to the apparent incomplete equilibration. However, the new interpretation of such zoning presented here does not rule out the application of barometric methods. All compositions across a zoning profile can be used, potentially, for pressure estimation, although not for example with the matrix mineral assemblage. It is of utmost importance that before the use of any thermobarometric method, the compositions and compositional variations of all phases in the rock should be carefully measured, rather than to measure only a few random points for use in calculating the  $P$ – $T$  conditions.

## ACKNOWLEDGEMENTS

Financial support for this project came from the European Commission (the Marie Curie Intra-European Fellowship Program) to LT. RP acknowledges support from ARC DP0987731. E.M. acknowledges the Alexander S. Onassis Public benefit foundation for financial support. We thank to T. Gerya, D. Schmid, M. Dabrowski and five anonymous reviewers for their constructive comments which improved to clarify the overall aim and the mechanical part of the manuscript. M. Brown is acknowledged for the careful editorial handling and patience.

## REFERENCES

- Ague, J.J. & Baxter, E.F., 2007. Brief thermal pulses during mountain building recorded by Sr diffusion in apatite and multicomponent diffusion in garnet. *Earth and Planetary Science letters*, **261**, 500–516.
- Barron, L. M., 2003. A simple model for the pressure preservation index of inclusions in diamond. *American Mineralogist*, **88**, 1615–1619.
- Brace, W.F., Ernst, W.G. & Kallberg, R.W., 1970. An Experimental Study of Tectonic Overpressure in Franciscan Rocks. *Geological Society of America Bulletin*, **81**, 1325–1338.
- Brady, J. B., 1983. Intergranular diffusion in metamorphic rocks. *American Journal of Science*, **283–A**, 181–200.
- Brown, W. L., & Willaime C., 1974. An explanation of exsolution orientations and residual strain in cryptoperthites. The Feldspars, Eds. W. S. MacKenzie and J. Zussman' 440–459.
- Caddick, M.J., Konopásek, J. & Thompson, A. B., 2010. Preservation of Garnet Growth Zoning and the Duration of Prograde Metamorphism. *Journal of Petrology*, **51**, 2327–2347.
- Camacho, A., Lee, J.K.W., Hensen, B.J. & Braun, J., 2005. Short-lived orogenic cycles and the eclogitization of cold crust by spasmodic hot fluids. *Nature*, **435**, 1191–1196.
- Carlson, W.D. & Johnson, C.D., 1991. Coronal reaction textures in garnet amphibolites of the Llano Uplift. *American Mineralogist*, **76**, 756–772.
- Carswell, D.A., Brueckner, H.K., Cuthbert, S.J., Mehta, K. & O'Brien, P.J., 2003. The timing of stabilisation and the exhumation rate for ultra-high pressure rocks in the Western Gneiss region of Norway. *Journal of Metamorphic Geology*, **21**, 601–612.
- Cherniak, 2010. Cation Diffusion in Feldspars In: Diffusion in minerals and melts. Eds.: Zhang, Y., Cherniak, DJ. *Reviews in Mineralogy and Geochemistry*, **72**, 691–733.
- Chopin, C. 1984. Coesite and pure pyrope in high-grade blueschists of the Western Alps: a first record and some consequences. *Contribution to Mineralogy Petrology*, **86**, 107–118.
- Chopin, C. 2003. Ultrahigh-pressure metamorphism: tracing continental crust into the mantle. *Earth and Planetary Science Letters*, **212**, 1–14.
- Connolly, J. A. D., 1990. Multivariable Phase Diagrams: An Algorithm Based on Generalized Thermodynamics. *American Journal of Science*, **290**, 666–718.
- Connolly, J. A. D., 2009. The geodynamic equation of state: what and how. *Geochemistry, Geophysics, Geosystems*, **10**, Q10014.
- Dahlen, F. A. 1992. Metamorphism of nonhydrostatically stressed rocks. *American Journal of Science*, **292**, 184–198.

- De Groot, S.R. & Mazur, P., 1962. Non–Equilibrium Thermodynamics. Amsterdam, North–Holland Pub. Co., New York, Interscience Publishers, 510pp.
- Dodson, M. H., 1973. Closure temperature in cooling geochronological and petrological systems. *Contributions to Mineralogy and Petrology*, **40**, 259–274.
- Enami, M., Nishiyama, T. & Mouri, T., 2007. Laser Raman microspectrometry of metamorphic quartz: A simple method for comparison of metamorphic pressures, *American Mineralogist*, **92**, 1303–1315.
- Ferguson, C. C. & Harvey, P. K., 1980. Porphyroblasts and “crystallization force”: Some textural criteria: Discussion. *Geol. Soc. Am. Bull.* **83**, 3839–3840.
- Fischer, F.D., Berveiller, M., Tanaka, K. and Oberaigner, E.R., 1994. Continuum mechanical aspects of phase transformations in solids, *Archive of Applied Mechanics*, **64**, 54–85,
- Fisher, G.W., 1973. Non–equilibrium thermodynamics as a model for diffusion–controlled metamorphic processes. *American Journal of Science*, **273**, 897–924.
- Fletcher, R. C. 1982 Coupling of diffusional mass transport and deformation in a tight rock. *Tectonophysics*, **83**, 275–291.
- Fletcher, R. C. & Merino, E., 2001. Mineral growth in rocks: Kinetic–rheological models of replacement, vein formation, and syntectonic crystallization. *Geochimica et Cosmochimica Acta*, **65**, 3733–3748.
- Franěk, J., Schulmann, K., Lexa, O., Ulrich, S., Štípská, P., Haloda, J. & Týcová, P., 2011. Origin of felsic granulite microstructure by heterogeneous decomposition of alkali feldspar and extreme weakening of orogenic lower crust during the Variscan orogeny. *Journal of Metamorphic Geology*, **29**, 103–130.
- Gibbs, J.W., 1906. The Scientific Papers: Thermodynamics. Dover Publications, 434pp.
- Gillet, P., Ingrin, J., & Chopin, C. (1984) Coesite in subducted continental crust: *P–T* history deduced from an elastic model. *Earth and Planetary Science Letters*, **70**, 426–436.
- Guiraud, M. & Powell, R., 2006. P–V–T relationships and mineral equilibria in inclusions in minerals. *Earth and Planetary Science Letters*, **244**, 683–694.
- Holland, T.J.B., Powell, R., 2003. Activity–composition relations for phases in petrological calculations: an asymmetric multicomponent formulation. *Contributions to Mineralogy and Petrology*, **145**, 492–501.
- Ji, S., Wirth, R., Rybacki, E. & Jiang, Z., 2000. High–temperature plastic deformation of quartz–plagioclase multilayers by layer–normal compression. *Journal of Geophysical Research*, **105**, 16 651–16 664.
- Joesten, R., 1977. Evolution of mineral assemblage zoning in diffusion metasomatism. *Geochimica et Cosmochimica Acta*, **41**, 649–670.
- Kamb, W.B., 1961. The thermodynamic theory of nonhydrostatically stressed solids. *Journal of Geophysical Research*, **66**, 259–271.
- Karato, S. 2003. The Dynamic Structure of the Deep Earth: An Interdisciplinary Approach. Princeton University Press. 264pp .
- Keller, L. M., Wirth, R., Rhede, D., Kunze, K. & Abart, R., 2008. Asymmetrically zoned reaction rims: assessment of grain boundary diffusivities and growth rates related to natural diffusion–controlled mineral reactions. *Journal of Metamorphic Geology*, **26**, 99–120.

- Korolyuk V.N. & Lepezin, G.G., 2009. The coefficients of heterovalent NaSi–CaAl interdiffusion of plagioclases. *Russian Geology and Geophysics*, **50**, 1146–1152.
- Kuiken, G.D.C., 1994. Thermodynamics of Irreversible Processes: Applications to Diffusion and Rheology. Wiley, Chapter 6, 458pp.
- Landau, L.D. & Lifshitz, E.M., 1987. Fluid Mechanics, Volume 6. Butterworth–Heinemann, second Edition, Chapter 6, 539pp.
- Lee, J.K., Earmme, Y.Y., Aaronson, H.I., Russell, K.C., 1980. Plastic relaxation of the transformation strain energy of a misfitting spherical precipitate: ideal plastic behaviour. *Metall. Trans. A*, **11**, 1837–1847.
- Liu M. & Yund R.A., 1992. NaSi–CaAl interdiffusion in plagioclase, *American Mineralogist*, **77**, 257–283.
- Liu, M., Kerschhofer, L., Mosenfelder, J. & Rubie, D.C., 1998. The effect of strain energy on growth rates during the olivine–spinel transformation and implications for olivine metastability in subducting slabs. *Journal of Geophysical Research*, **103**, 23897–23909.
- Loomis, T.P., 1978. Multicomponent diffusion in garnet: I. Formulation of isothermal models. *American Journal of Science*, **278**, 1099–1118.
- Mancktelow, N. S., 2008. Tectonic pressure: Theoretical concepts and modelled examples. *Lithos*, **103**, 149–177.
- Markl, G., Foster, C. T. & Bucher, K., 1998. Diffusion–controlled olivine corona textures in granitic rocks from Lofoten, Norway: calculation of Onsager diffusion coefficients, thermodynamic modelling and petrological implications. *Journal of Metamorphic Geology*, **16**, 607–623.
- Milke, R., & Heinrich, W., 2002. Diffusion–controlled growth of wollastonite rims between quartz and calcite: comparison between nature and experiment. *Journal of Metamorphic Geology*, **20**, 467–480.
- Milke, R., Abart, R., Kunze, K., Koch–Muller, M., Schmid, D. W. & Ulmer, P., 2009. Matrix rheology effects on reaction rim growth I: evidence from orthopyroxene rim growth experiments. *Journal of Metamorphic Geology*, **27**, 71–82.
- Moghadam, R. H., Trepmann, C. A., Stoeckert, B. & Renner, J., 2010. Rheology of synthetic omphacite aggregates at high pressure and high temperature. *Journal of Petrology*, **51**, 921–945.
- Morris, S. J. S., 1992. Stress Relief during Solid–State Transformations in Minerals. *Proceedings: Mathematical and Physical Sciences*, **436**, 203–216.
- Morris, S. J. S., 2002. Coupling of interface kinetics and transformation–induced strain during pressure–induced solid–solid phase changes. *Journal of the Mechanics and Physics of Solids*, **50**, 1363–1395.
- Mosenfelder, J.L., Connolly, J.A.D., Rubie, D.C. & Liu, M., 2000. Strength of (Mg; Fe)<sub>2</sub> wadsleyite determined by relaxation of transformation stress. *Phys. Earth Planet. Int.* **120**, 63–78.
- Moulas, E., Podladchikov, Y.Y., Aranovich, L.Y. & Kostopoulos, D., 2013. The Problem of Depth in Geology: when Pressure does not Translate into Depth. *Petrology*, **21**, 1–12.
- Müller, I. & Weiss, W. (2012) Thermodynamics of irreversible processes—past and present. *The European Physical Journal H*, **37**, 139–236.



- Neusser, G., Abart, R., Fischer, F.D., Harlov, D. & Norberg, N., 2012. Experimental Na/K exchange between alkali feldspar and an NaCl–KCl salt melt: chemically induced fracturing and element partitioning. *Contributions to Mineralogy and Petrology*, DOI 10.1007/s00410-012-0741-9.
- O'Brien, P.J. & Ziemann, M.A., 2008. Preservation of coesite in exhumed eclogite: insights from Raman mapping. *European Journal of Mineralogy*, **20**, 827–834.
- Parkinson, C.D., & Katayama, I., 1999. Present-day ultrahigh-pressure conditions of coesite inclusions in zircon and garnet: Evidence from laser Raman microspectroscopy. *Geology*, **27**, 979–982.
- Paterson, M.S., 1973. Nonhydrostatic thermodynamics and its geologic applications. *Reviews of Geophysics and Space Physics*, **11**, 355–389.
- Powell, R., Guiraud, M. & White, R.W., 2005. Truth and beauty in metamorphic mineral equilibria: conjugate variables and phase diagrams. *Canadian Mineralogist*, **43**, 21–33.
- Pryer, L.L. & Robin, P.Y.F., 1996. Differential stress control on the growth and orientation of flame perthite: a palaeostress–direction indicator. *Journal of Structural Geology*, **18**, 1151–1166.
- Robertson, E.C., 1955. Experimental study of the strength of rocks. *Bulletin of the geological Society of America*, **66**, 1275–1314.
- Robin, P.Y.F., 1974. Stress and strain in cryptoperthite lamellae and the coherent solvus of alkali feldspars. *American Mineralogist*, **59**, 1299–1318.
- Rosenfeld, J. L., 1969. Stress effects around quartz inclusions in almandine and the piezothermometry of coexisting aluminum silicates. *American Journal of Science*, **267**, 317–351.
- Rutter, E.H., 1976. The kinetics of rock deformation by pressure solution. *Philos Trans R Soc London A*, **283**, 203–219.
- Rybacki, E. & Dresen, G., 2000. Dislocation and diffusion creep of synthetic anorthite aggregates. *Journal of Geophysical Research*, **105**, 26 017–26 036.
- Rybacki, E. & Dresen, G., 2004. Deformation mechanism maps for feldspar rocks. *Tectonophysics*, **382**, 173–187.
- Schmid, D. W., Abart, R., Podladchikov, Y. Y. & Milke, R., 2009. Matrix rheology effects on reaction rim growth II: coupled diffusion and creep model. *Journal of Metamorphic Geology*, **27**, 83–91.
- Smith, D.C., 1984. Coesite in clinopyroxene in the Caledonides and its implications for geodynamics. *Nature*, **310**, 641–644.
- Stephansson, O., 1974. Stress-induced diffusion during folding. *Tectonophysics*, **22**, 233–251.
- Štípská, P., Powell, R., White, R.W. & Baldwin, J.A., 2010. Using calculated chemical potential relationships to account for coronas around kyanite: an example from the Bohemian Massif. *Journal of Metamorphic Geology*, **28**, 97–116.
- Tajčmanová, L., Konopásek, J. & Connolly, J.A.D., 2007. Diffusion-controlled development of silica-undersaturated domains in felsic granulites of the Bohemian Massif (Variscan belt of Central Europe). *Contributions to Mineralogy and Petrology*, **153**, 237–250.

- Tajčmanová, L., Abart, R., Neusser, G. & Rhede, D., 2011. Growth of decompression plagioclase rims around metastable kyanite from high–pressure felsic granulites (Bohemian Massif). *Journal of Metamorphic Geology*, **29**, 1003–1018.
- Tajčmanová, L., Abart, R., Wirth, R. Habler, G. & Rhede D., 2012. Intracrystal microtextures in alkali feldspars from fluid deficient felsic granulites: A chemical and TEM study. *Contribution to Mineralogy and Petrology*, **164**, 715–729.
- Truesdell, C., 1962. Mechanical Basis of Diffusion. *The Journal of Chemical Physics*, **37**, 2336–2344.
- Van der Molen, I. & van Roermund, H.L.M., 1986. The pressure path of solid inclusions in minerals: The retention of coesite inclusions during uplift. *Lithos*, **19**, 317–324.
- Wheeler, J., 1987. The significance of grain–scale stresses in the kinetics of metamorphism. *Contributions to Mineralogy and Petrology*, **97**, 397–404.
- Willaime, C. & Gandais, M. 1972. Study of exsolution in alkali feldspars. Calculation of elastic stresses inducing periodic twins. *Physica Status Solidi (a)*, **9**, 529–539.
- Yarushina, V.M. & Podladchikov, Y.Y., 2010. Plastic yielding as a frequency and amplitude independent mechanism of seismic wave attenuation. *Geophysics*, **75**, 51–63.
- Ye, K., Liou, J.B., Cong, B., & Maruyama, S. 2001. Overpressures induced by coesite–quartz transition in zircon. *American Mineralogist*, **86**, 1151–1155.
- Yu, H.S. & Houlsby, G.T., 1991. Finite cavity expansion in dilatant soils: loading analysis. *Geotechnique*, **41**, 173–183.
- Yu, H.S., 2000. Cavity Expansion Methods in Geomechanics. Springer, 1st edition, 385pp.
- Yund, R., 1986. Interdiffusion of NaSi–CaAl in peristerite. *Physics and chemistry of minerals*, **13**, 11–16.
- Zhang, Y. & Cherniak, D.J., 2010. Diffusion in minerals and melts. *Reviews in Mineralogy and Geochemistry*, **72**, doi:10.2138/rmg.2010.72.0.
- Zhang, R.Y. & Liou, J.G., 1997. Partial transformation of gabbro to coesite–bearing eclogite from Yangkou, the Sulu terrane, eastern China. *Journal of Metamorphic Geology*, **15**, 183–202.
- Zhang, Y.X., 1998. Mechanical and phase equilibria in inclusion–host systems. *Earth and Planetary Science Letters*, **157**, 209–222.

## FIGURE AND TABLE CAPTIONS

**Fig. 1: a)** The time required for equilibrium at a length scale of 1mm at 800°C for different diffusion–type processes, diffusion coefficients for different elements and stress decay ( $t_{\sigma}$ ; Maxwell relaxation time;  $t_{\sigma} = \text{viscosity/elastic modulus}$ ). **b)** The time dependence of equilibration rates on temperature. The thick grey line separates an apparently slow and a relatively fast region. Diffusion coefficients for components are taken from Zhang & Cherniak (2010), specifically  $1 \times 10^{-7/-9}$  [ $\text{m}^2 \text{s}^{-1}$ ] for  $\text{H}_2\text{O}$ ;  $1 \times 10^{-9/-13}$  [ $\text{m}^2 \text{s}^{-1}$ ] for  $\text{K}_2\text{O}$ ,  $\text{Na}_2\text{O}$ ,  $\text{Ba}_2\text{O}$ ;  $1 \times 10^{-16/-22}$  [ $\text{m}^2 \text{s}^{-1}$ ] for  $\text{FeO}$ ,  $\text{MgO}$ ,  $\text{MnO}$ ,  $\text{CaO}$  and  $1 \times 10^{-17/-22}$  [ $\text{m}^2 \text{s}^{-1}$ ] for  $\text{Al}_2\text{O}_3$ ,  $\text{SiO}_2$ . The range of viscosity,  $10^{12}$ – $10^{26}$  Pas, is from Karato (2003) and the elastic modulus corresponds to  $10^{10}$  Pa.

**Fig. 2:** A force balanced stress–area relationship. **a)** Piston cylinder apparatus; **b)** Multi–anvil apparatus with stresses varying with radial coordinate  $r$ .  $P$  is pressure,  $\sigma$  is stress,  $F$

is force acting upon the area  $A$ . Force balance requires equality of forces but not equality of stresses if areas are different.

**Fig. 3:** **a)** Common mechanical view of a weak polycrystalline matrix.  $P$  is pressure,  $\sigma_{max}$  and  $\sigma_{min}$  are maximum and minimum stress respectively. **b)** A cross-section through a host grain with a high-pressure inclusion. This sketch represents an elastic rheology.  $P$  is pressure,  $\sigma_{max}$  corresponds to radial stress  $\sigma_r$ ,  $\sigma_{min}$  to circumferential stress  $\sigma_\theta$  and  $\bar{\sigma}$  is a mean stress being constant across the host in the elastic regime.  $\sigma_{max} - \sigma_{min}$  is differential stress in the host and  $r$  is a radial coordinate. **c)** A mechanical model for a high-pressure inclusion surrounded by a polycrystalline rim composed of strong grains separated by weak grain boundaries (multi-anvil model).  $\sigma_{rGB}$  and  $\sigma_{\theta GB}$  are radial and circumferential stresses at weak grain boundaries.  $\sigma_\theta$ ,  $\sigma_{rGB}$  and  $\sigma_{\theta GB}$  are equal to low pressure in the matrix due to the weakness of the grain boundaries. **d)** A cross-section through the mechanical model in Fig. 3c.

**Fig. 4:** Schematic figure of **(a)** distribution of pressure and molar fraction of a system component in a binary solid-solution mineral grown between a high-pressure (HP) mineral grain and a low-pressure (LP) matrix. **(b)**  $\frac{g}{M}$ - $X$  diagram ( $X=X_A/(X_A+X_B)$ ) for constant temperature portraying the equilibrium situation with varying pressure, represented as a series of pressure steps ( $P1-P7$ ). Each step is represented by a parabola portraying the path of a point traversing a 3D  $\frac{g}{M}$ - $P$ - $X$  surface for the mineral.

$\frac{\mu_A}{M_A} - \frac{\mu_B}{M_B}$  and  $\frac{g}{M}$  stand for the chemical potentials and a Gibbs free energy converted to molar mass respectively.

**Fig. 5:** Sketch of a thin section in which two different microstructures, perthite and the plagioclase rim on kyanite, may be interpreted to record pressure heterogeneities.

**Fig. 6:** Perthitic alkali feldspar from a slowly-cooled felsic granulite. Two generations of exsolution lamellae are portrayed. A first generation of thicker precipitates, already incoherent, and a second coherent generation of tiny film lamellae. The rectangular outline represents the top sketch, which shows a map of induced stresses in exsolution lamellae indicated for different crystallographic directions. For details of the evolution of the exsolution lamellae, see Tajčmanová *et al.* (2012).

**Fig. 7:** Plagioclase rim around kyanite from felsic granulite. **a)** Enclosed in large perthitic alkali feldspar. **b)** In polycrystalline matrix.

**Fig. 8:** **(a)** A diagram showing isopleths of differences in mass chemical potentials across the plagioclase rim. **(b)** Calculated mass  $(\frac{\mu_{An}}{M_{An}} - \frac{\mu_{Ab}}{M_{Ab}})$  chemical potential differences across the plagioclase rim at isobaric conditions of 10 kbar (isoB) and under the inferred pressure variations (Pvar).

**Fig. 9:** (a) Concentration profile across the plagioclase rim. (b) Density profile across the plagioclase rim. (c) Pressure variation across the plagioclase rim calculated with Eq. 10 (see text).